Chemical Modification of Transition Metal Upconversion Properties: Exchange Enhancement of Ni^{2+} Upconversion Rates in Ni^{2+}:$RbMnCl_3$

Oliver S. Wenger, Daniel R. Gamelin, and Hans U. Güdel*

Departement für Chemie und Biochemie
Universität Bern, Freiestrasse 3, CH-3000 Bern 9, Switzerland

Received March 20, 2000

Upconversion (UC) is an efficient way to convert near-infrared (NIR) light into visible (VIS) luminescence. Several lasers,[1] imaging materials devices,[2] and IR quantum counting devices[3] have been reported based on UC pumping mechanisms. The majority of UC materials involve rare-earth (RE) ions since these usually luminesce from various excited states. The research field of transition metal (TM) UC on the other hand is very young and much less explored.[4] Recently, UC has been observed in Ti^{2+},[5] Ni^{2+},[6] Mo^{3+},[7] Re^{4+},[8] and Os^{4+}.[9] The advantage of such TM upconverters when compared to RE UC ions is their sensitivity toward their ligand field environments: it allows the modification of UC properties by chemical means. This advantage has been exploited in this study. We show that, compared to Ni^{2+} ions in the diamagnetic $CsCdCl_3$ host, the Ni^{2+} UC efficiency is significantly enhanced via $Ni^{2+}-Mn^{2+}$ exchange interactions in the isostructural $RbMnCl_3$ host. Such a controlled chemical modification of UC efficiencies is unprecedented in any previously reported material and represents a significant advance in the research field of UC.

Figure 1a shows the energy levels for d^8 ions in octahedral coordination as a function of the ligand field strength.[10] For both samples considered in this study the resulting energy level sequence is that at the vertical dashed line, and is presented in Figure 1b. Ni^{2+} emits not only from the $^3T_{2g}$ first excited state but also from the $^1T_{2g}$ higher excited state in a variety of host lattices, including chlorides, fluorides, and oxides.[11,12] The Ni^{2+} UC mechanism in chlorides is shown in Figure 1b: $^3A_{2g} \rightarrow {}^1E_g$ ground-state absorption (GSA) (up arrow) is followed by rapid nonradiative multiphonon relaxation to the metastable $^3T_{2g}$ first excited state (curly down arrow) and $^3T_{2g} \rightarrow {}^1T_{2g}$ excited state absorption (ESA) (up arrow). From there, emission occurs to all energetically lower lying levels. Only that to the ground state is indicated (down arrow). Since both GSA and ESA are formally spin-forbidden transitions, their cross-sections are small. As a consequence, the UC process in diamagnetic host materials such as $CsCdCl_3$ is relatively inefficient.

Figure 2 presents 15 K axial GSA spectra of (a) 10% Ni^{2+}:$CsCdCl_3$ and (b) 10% Ni^{2+}:$RbMnCl_3$.[13] All bands in spectrum a are due to Ni^{2+} and are assigned according to Figure 1. In spectrum b the same Ni^{2+} transitions are superimposed upon Mn^{2+} $^4T_{1g}$ and $^4T_{2g}$ absorption bands centered at 19 200 and 22 400 cm^{-1}, respectively. In the 0−17 500 cm^{-1} window Mn^{2+} is spectroscopically innocent. In this energy region the most striking difference between the two absorption spectra is the intensity of the Ni^{2+} ^1E_g band. Whereas the intensities of the spin-allowed

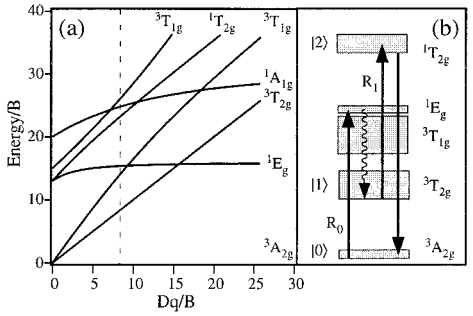

Figure 1. (a) d^8 Tanabe-Sugano energy-level diagram. The vertical dashed line represents the ligand field strength in Ni^{2+}-doped $CsCdCl_3$ and $RbMnCl_3$. (b) Summary of the UC processes in Ni^{2+}-doped chlorides. The solid arrows represent the radiative processes of GSA, ESA, and luminescence, and the curly arrow indicates nonradiative multiphonon relaxation.

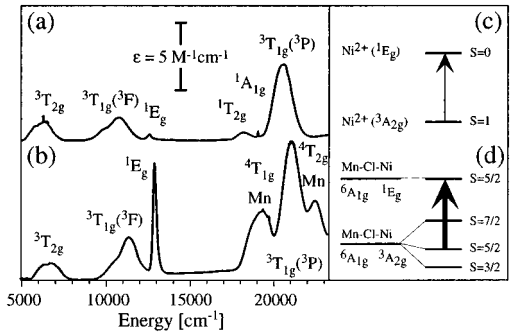

Figure 2. 15 K absorption spectra of (a) 10% Ni^{2+}:$CsCdCl_3$ and (b) 10% Ni^{2+}:$RbMnCl_3$. Energy level schemes of the Ni^{2+}-centered $^3A_{2g} \rightarrow {}^1E_g$ transition for (c) an isolated Ni^{2+} ion in $CsCdCl_3$ and (d) a $Ni^{2+}-Mn^{2+}$ pair in Ni^{2+}:$RbMnCl_3$.

$^3A_{2g} \rightarrow {}^3T_{2g}$ and $^3A_{2g} \rightarrow {}^3T_{1g}$ (^3F) transitions are similar in both spectra, the oscillator strength of the formally spin-forbidden $^3A_{2g} \rightarrow {}^1E_g$ transition is 20 times higher in Ni^{2+}:$RbMnCl_3$ than in Ni^{2+}:$CsCdCl_3$.

This enhancement derives from $Ni^{2+}-Mn^{2+}$ exchange interactions, which introduce new spin-allowedness into both the GSA and ESA transitions through the so-called Tanabe intensity mechanism,[14] and it is unprecedented for Ni^{2+}. Although $RbMnCl_3$ is a three-dimensional antiferromagnet at 15 K,[15] the most relevant interactions are between the Ni^{2+} and its nearest neighbor Mn^{2+} ions. For simplicity we illustrate the exchange enhancement for the Ni^{2+}-centered $^3A_{2g} \rightarrow {}^1E_g$ transition using a dimer picture. In a $Ni^{2+}-Mn^{2+}$ dimer the ground state is [Ni^{2+} ($^3A_{2g}$), Mn^{2+} ($^6A_{1g}$)] with spin levels of $S_{dimer} = {}^3/_2, {}^5/_2, {}^7/_2$. The Ni^{2+}-centered ^1E_g excited state has $S_{Ni} = 0$ and therefore the corresponding dimer excited state has only a $S_{dimer} = {}^5/_2$ spin level. For an antiferromagnetic interaction between Ni^{2+} and Mn^{2+} this leads to the energy level scheme in Figure 2d. There is a formally spin-allowed

(1) Joubert, M. F. *Opt. Mater.* **1999**, *11*, 181−203.
(2) Downing, E.; Hesselink, L.; Ralston, J.; Macfarlane, R. *Science* **1996**, *273*, 1185−1189.
(3) Chivian, J. S.; Case, W. E.; Eden, D. D. *Appl. Phys. Lett.* **1979**, *35*, 124−125.
(4) Gamelin, D. R.; Güdel, H. U. *Acc. Chem. Res.* **2000**, *33*, 235−242.
(5) Jacobsen, S. M.; Güdel, H. U. *J. Lumin.* **1989**, *43*, 125−137.
(6) Oetliker, U.; Riley, M. J.; May, P. S.; Güdel, H. U. *J. Lumin.* **1992**, *53*, 553−556.
(7) Gamelin, D. R.; Güdel, H. U. *J. Am. Chem. Soc.* **1998**, *120*, 12143−12144.
(8) Gamelin, D. R.; Güdel, H. U. *Inorg. Chem.* **1999**, *38*, 5154−5164.
(9) Wermuth, M.; Güdel, H. U. *J. Am. Chem. Soc.* **1999**, *121*, 10102−10111.
(10) Tanabe, Y.; Sugano, S. *J. Phys. Soc. Jpn.* **1954**, *9*, 753−766.
(11) May, P. S.; Güdel, H. U. *J. Chem. Phys.* **1991**, *95*, 6343−6354.
(12) Moncorgé, R.; Benyattou, T. *Phys. Rev. B* **1988**, *37*, 9186−9196.

(13) Single crystals of 10% doped $CsCdCl_3$ and $RbMnCl_3$ were grown by the Bridgman technique using stoichiometric amounts of CsCl/RbCl, $MnCl_2$, and $NiCl_2$. Absorption spectra were measured on a Cary 5e spectrometer with closed-cycle cryogenic cooling. Luminescence spectra were excited with an Ar^+ laser (Ion Laser Technology). For UC luminescence and excitation two Ti:sapphire lasers (Spectra Physics 3900S) were used. The sample luminescence was dispersed by either a $^3/_4$ m single monochromator (Spex 1702) or a 0.85 m double monochromator (Spex 1402) and detected by a PMT (RCA C31034). For lifetime measurements the laser beam was chopped by an acoustooptic modulator (Coherent 305, Stanford Research DS 345 function generator), and the signals were recorded with a multichannel scaler (SR 430). Sample cooling was achieved with a He flow technique.

(14) Ferguson, J.; Guggenheim, H. J.; Tanabe, Y. *J. Phys. Soc. Jpn.* **1966**, *21*, 692−704.
(15) Melamud, M.; Makovsky, J.; Shaked, H.; Shtrikman, S. *Phys. Rev. B* **1971**, *3*, 821.

10.1021/ja000979o CCC: $19.00
Published on Web 07/14/2000

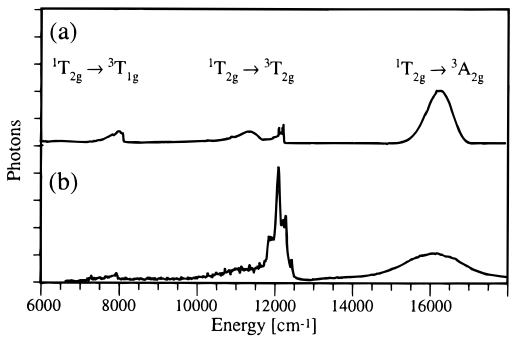

Figure 3. 15 K unpolarized emission spectra of (a) 10% Ni^{2+}:$CsCdCl_3$ and (b) 10% Ni^{2+}:$RbMnCl_3$, scaled to an equal integrated $^1T_{2g} \rightarrow {}^3A_{2g}$ emission intensity.

$S_{dimer} = {}^5/_2 \rightarrow {}^5/_2$ transition which dominates the $^3A_{2g} \rightarrow {}^1E_g$ oscillator strength in the Ni^{2+}:$RbMnCl_3$ absorption spectrum (see solid arrow in Figure 2d). This transition is thermally activated, with an intensity maximum around 50 K, in agreement with the fact that $S_{dimer} = {}^5/_2$ is not the ground state in Figure 2d. Although the presented dimer picture is too simple to model this temperature dependence quantitatively, Figure 2d clearly illustrates the origin of the enhanced intensity in Ni^{2+}:$RbMnCl_3$ relative to Ni^{2+}:$CsCdCl_3$. A characteristic of the Tanabe intensity mechanism is that pure spin-flip transitions involving no changes in electron orbital occupancies are influenced most dramatically by exchange interactions, while spin-allowed transitions essentially stay unaffected. Spin-forbidden transitions involving an orbital promotion represent an intermediate case. These trends are observed in Figure 2b, where the pure spin-flip $^3A_{2g} \rightarrow {}^1E_g$ transition shows by far the largest change in intensity.

In $CsCdCl_3$, the Ni^{2+} ions substitute for only one of the two crystallographically distinct sites.[16] We assume that this is also the case in the isostructural $RbMnCl_3$.[17] The Ni^{2+} site is part of a trigonally distorted $[NiCl_6]^{4-}$ octahedral unit which shares a face with one $[MnCl_6]^{4-}$ unit as well as a corner with a second $[MnCl_6]^{4-}$ unit. Consequently, in Ni^{2+}:$RbMnCl_3$, $Ni^{2+}-Mn^{2+}$ exchange interactions can in principle occur by both pathways. However, the spin density of the Ni^{2+} ion is located only in the e_g-set of d-orbitals, and consequently the corner-sharing superexchange pathway with a $Ni^{2+}-Cl^--Mn^{2+}$ angle close to 180° is dominant. Parallel studies on Ni^{2+}:$CsMnCl_3$, where the $Ni^{2+}-Cl^--Mn^{2+}$ bridging angle is close to 90°,[18] show much smaller changes in ^1E_g intensity relative to Ni^{2+}:$CsCdCl_3$. These findings are in agreement with previous studies on $Ni^{2+}-Mn^{2+}$ exchange interactions in other lattices.[19,20]

Figure 3 presents 15 K downconversion luminescence spectra of (a) 10% Ni^{2+}:$CsCdCl_3$ and (b) 10% Ni^{2+}:$RbMnCl_3$ obtained with 20 486 and 20 981 cm^{-1} excitation, respectively.[13] The total emission intensity in Figure 3b is about an order of magnitude smaller than that in Figure 3a. We ascribe this to nonradiative quenching processes by traces of Mn^{3+} in $RbMnCl_3$. Of importance for our discussion are the intensity ratios in the two spectra, and for this purpose the spectra were normalized to an equal $^1T_{2g} \rightarrow {}^3A_{2g}$ emission intensity, which is hardly affected by exchange interactions. This band is slightly broadened in the 10% Ni^{2+}:$RbMnCl_3$ spectrum due to the presence of about 10% $^4T_{1g} \rightarrow {}^6A_{1g}$ Mn^{2+} emission. The striking feature in Figure 3 is the enhancement by an order of magnitude of the highest-energy components of the $^1T_{2g} \rightarrow {}^3T_{2g}$ emission in 10% Ni^{2+}:$RbMnCl_3$ at about 12 000 cm^{-1}. Similar to the enhancement of the $^3A_{2g} \rightarrow {}^1E_g$ absorption transition discussed above, this is ascribed to an exchange mechanism in the magnetic lattice. The reverse transition $^3T_{2g} \rightarrow {}^1T_{2g}$ corresponds to the ESA step in our upconversion process (see Figure 1b). The absorption cross-sections at the maxima of both excitation steps $^3A_{2g} \rightarrow {}^1E_g$ (GSA) and $^3T_{2g} \rightarrow {}^1T_{2g}$ (ESA) are thus each enhanced by about an order of magnitude by exchange in the $RbMnCl_3$ host. In Figure 1b the levels $^3A_{2g}$, $^3T_{2g}$, and $^1T_{2g}$ are labeled $|0\rangle$, $|1\rangle$, and $|2\rangle$, respectively. The rate at which a level $|i\rangle$ is depopulated by laser excitation is

$$R_i = cP\sigma_i N_i \tag{1}$$

where c is a constant, P the laser power, and N_i the population density. σ_i is the absorption cross-section at the laser wavelength. The differential rate equation for the population density N_1 of the $^3T_{2g}$ intermediate state is

$$dN_1/dt = R_0 - R_1 - k_1 N_1 + k_2 N_2 \tag{2}$$

where the first two terms represent $^3T_{2g}$ population by GSA and depopulation by ESA, respectively. The third term represents decay of the $^3T_{2g}$ population to the ground state with the decay rate constant k_1. In the last term all the processes that re-populate $^3T_{2g}$ from the $^1T_{2g}$ higher excited state with a total rate constant k_2 are summarized. In the low power limit R_1 is small and consequently the population density N_2 is negligible. Under steady-state conditions, N_1 is then

$$N_1 = R_0/k_1 \tag{3}$$

Substitution of this expression in eq 1 leads to the following result for the rate R_1 with which the upper emitting $^1T_{2g}$ level is populated

$$R_1 = c^2P^2N_0[(\sigma_0 \cdot \sigma_1)/k_1] \tag{4}$$

R_1 is the upconversion rate we are interested in. The first three factors in eq 4 are essentially the same in the two host lattices. σ_0 and σ_1 are enhanced by factors of about 20 and 10 in 10% Ni^{2+}:$RbMnCl_3$ due to the exchange mechanism. The decay rate constants k_1 at 15 K are 175 and 130 s^{-1} in 10% Ni^{2+}:$RbMnCl_3$ and 10% Ni^{2+}:$CsCdCl_3$, respectively. We thus calculate a total enhancement of the upconversion rate by a factor of 150 in the magnetic lattice. Considering the experimental uncertainty this is in very good agreement with the experimentally determined enhancement factor of 80. This value was obtained from a comparison of UC luminescence intensities in 10% Ni^{2+}:$CsCdCl_3$ and 10% Ni^{2+}:$RbMnCl_3$ after two-color excitation with one laser in resonance with the GSA maxima and a second laser in resonance with the ESA maxima.

In summary, we have demonstrated a new way to tune Ni^{2+} UC rates by chemical variation. Exchange enhancement of Ni^{2+} absorption cross-sections in Ni^{2+}:$RbMnCl_3$ leads to an increased UC efficiency compared to the isostructural but diamagnetic $CsCdCl_3$ host lattice. We have demonstrated that exchange interactions between TM ions can be exploited for the modification of their UC properties, in particular they allow us to overcome the problem of weak spin-forbidden absorption transitions. In this sense the present study outlines a principle that is generally applicable to TM UC systems where the UC pathway is inhibited by spin selection rules. This study also demonstrates the broader principle of environmental control of TM UC properties using chemical means to take advantage of the accessibility of their spectroscopically active d-orbitals. This is in contrast to RE UC systems where, due to the shielded nature of the spectroscopically active f-orbitals, such a controlled modification of the UC properties by means of chemistry is impossible.

Acknowledgment. The authors thank Rafael Valiente for valuable discussions. This research has been supported by the Swiss National Science Foundation.

JA000979O

(16) Chang, J. R.; McPherson, G. L.; Atwood, J. L. *Inorg. Chem.* **1975**, *14*, 3079−3085.
(17) Goodyear, J.; Steigman, G. A.; Ali, M. E. *Acta Crystallogr.* **1977**, *B33*, 256−258.
(18) Wenger, O. S.; Güdel, H. U. Submitted for publication.
(19) Ferguson, J.; Guggenheim, H. J.; Tanabe, Y. *Phys. Rev. Lett.* **1965**, *14*, 737−738.
(20) Ferguson, J.; Guggenheim, H. J.; Tanabe, Y. *Phys. Rev.* **1967**, *161*, 207−212.